Quantifying liver-toxic responses from dose-dependent chemical exposures using a rat genome-scale metabolic model

Venkat R. Pannala [1,2,*], Archana Hari[1,2], Mohamed Diwan M. AbdulHameed[1,2], Michele R. Balik-Meisner[3], Deepak Mav[3], Dhiral P. Phadke[3], Elizabeth H. Scholl[3], Ruchir R. Shah[3], Scott S. Auerbach [4], Anders Wallqvist[1,*]

[1]Department of Defense Biotechnology High Performance Computing Software Applications Institute, Telemedicine and Advanced Technology Research Center, U.S. Army Medical Research and Development Command, Fort Detrick, MD 21702, United States
[2]The Henry M. Jackson Foundation for the Advancement of Military Medicine, Inc., Bethesda, MD 20817, United States
[3]Sciome LLC, Research Triangle Park, NC 27709, United States
[4]Division of Translational Toxicology, National Institute of Environmental Health Sciences, Research Triangle Park, NC 27709, United States

*Corresponding authors: Venkat R. Pannala, Department of Defense Biotechnology High Performance Computing Software Applications Institute, Telemedicine and Advanced Technology Research Center, U.S. Army Medical Research and Development Command, FCMR-TT, 504 Scott Street, Fort Detrick, MD 21702-5012, United States. Email: vpannala@bhsai.org; Anders Wallqvist, Department of Defense Biotechnology High Performance Computing Software Applications Institute, Telemedicine and Advanced Technology Research Center, U.S. Army Medical Research and Development Command, FCMR-TT, 504 Scott Street, Fort Detrick, MD 21702-5012, United States. Email: sven.a.wallqvist.civ@health.mil

Abstract

Because the liver plays a vital role in the clearance of exogenous chemical compounds, it is susceptible to chemical-induced toxicity. Animal-based testing is routinely used to assess the hepatotoxic potential of chemicals. Although large-scale high-throughput sequencing data can indicate the genes affected by chemical exposures, we need system-level approaches to interpret these changes. To this end, we developed an updated rat genome-scale metabolic model to integrate large-scale transcriptomics data and utilized a chemical structure similarity-based ToxProfiler tool to identify chemicals that bind to specific toxicity targets to understand the mechanisms of toxicity. We used high-throughput transcriptomics data from a 5-day in vivo study where rats were exposed to different non-toxic and hepatotoxic chemicals at increasing concentrations and investigated how liver metabolism was differentially altered between the non-toxic and hepatotoxic chemical exposures. Our analysis indicated that the genes identified via toxicity target analysis and those mapped to the metabolic model showed a distinct gene expression pattern, with the majority showing upregulation for hepatotoxicants compared with non-toxic chemicals. Similarly, when we mapped the metabolic genes at the pathway level, we identified several pathways in carbohydrate, amino acid, and lipid metabolism that were significantly upregulated for hepatotoxic chemicals. Furthermore, using our system-level integration of gene expression data with the rat metabolic model, we could differentiate metabolites in these pathways that were systematically elevated or suppressed due to hepatotoxic versus non-toxic chemicals. Thus, using our combined approach, we were able to identify a set of potential gene signatures that clearly differentiated liver toxic responses from non-toxic chemicals, which helped us identify potential metabolic pathways and metabolites that are systematically associated with the toxicant exposure.

Keywords: liver toxicity; high-throughput transcriptomics; metabolite predictions; environmental chemicals; chemical structure-based analysis; toxicity targets

The liver plays a central role in a wide range of physiological functions, including maintaining systemic metabolic homeostasis and synthesizing lipids, carbohydrates, and most plasma proteins (Jones 2016). In addition, it synthesizes and excretes bile acids, which are critical for the normal uptake of vitamins and lipids as well as for the excretion of xenobiotics (Corless and Middleton 1983). Furthermore, the liver is one of the key organs for xenobiotic metabolism, acting as a physical and biochemical barrier between the absorbed xenobiotics and the systemic circulation due to its strategic location and possessing a very high capacity for phases I and II metabolic processes involved in the clearance of xenobiotics. Therefore, as the main detoxifying organ in the body, the liver is prone to toxic injury, which leads to disruption of its normal functionalities and several liver diseases, such as non-alcoholic fatty liver disease, fibrosis, cirrhosis, and liver cancer, that are serious threats to public health (Baffy et al. 2012; Byass 2014; Benedict and Zhang 2017). Indeed, liver injury is a common reason for the termination of preclinical testing of new drugs and for the withdrawal of approved drugs from the market (Regev 2014; Seeff 2015). In addition, many common workplace and environmental chemicals are associated with liver toxicity (Pond 1982; Tolman and Sirrine 1998; Cave et al. 2010; Al-Eryani et al. 2015; Committee et al. 2019).

As the liver is the first line of defense against many potentially harmful xenobiotics, we need methodologies and tools to achieve a detailed description of the biological mechanisms that

contribute to liver injury as well as a means to predict injury occurrence. In classic toxicology testing, the liver toxicity of a potential toxic chemical is determined using in vivo studies based on detailed histopathological examination of tissue specimens after prolonged and repeated rodent exposures (OECD 1994). However, these long-term animal studies are ethically disputed, costly, time-consuming, and may not be feasible for a large number of chemicals (Van Norman 2019; Kiani et al. 2022). To circumvent this problem, the National Toxicology Program (NTP) proposed a novel high-throughput transcriptomics platform (HTT) combined with short-term in vivo 5-day rat exposure studies for understanding a quantitative estimate of hazard, as a bioactivity-based bridge between traditional apical endpoints and the HTT data generated from the in vitro assays (Ramaiahgari et al. 2019; Gwinn et al. 2020). These studies were able to determine the lowest transcriptional benchmark dose (BMD) estimated from HTT, which was within a factor of 5 of the values estimated from the traditional apical endpoints obtained via longer term studies, and suggested that the 5-day rat in vivo model can be used as a rapid approach for estimating BMD values (Gwinn et al. 2020). Use of these HTT data types should increase the efficiency of chemical testing and prioritization, reduce the number of animals used for testing, and allow for better allocation of resources to chemicals with the greatest potential for human health risk.

Toxicogenomic dose-response studies generate large volumes of omics data, and their complexity requires advanced computational tools to determine patterns of interest among several variables to understand the mechanisms of toxicity. In general, dimension-reduction methods are routinely used to describe and visualize these large multidimensional datasets, but they do not provide functional interpretation of the data. Alternatively, gene enrichment-based methodologies, which allow for the identification of biological modules that provide an overview of the studied biological modulations, can be used to identify putative markers for adverse health effects (Tawa et al. 2014; Nguyen et al. 2019; Karp et al. 2021; Pannala et al. 2023). However, these methods were developed based on arbitrary thresholds and might differ depending on the selected toxic chemical exposure database (Ganter et al. 2006; Igarashi et al. 2015). Furthermore, although these methods provided functional interpretation and potential biomarkers, the underlying mechanisms leading to liver injury still remain elusive. It is therefore difficult to track the onset and progression of injury or to translate the results between species to diagnose and design effective therapeutic countermeasures for toxic effects. Liver injury outcomes may be better predicted if we could understand how liver metabolism is altered as a result of toxicity. However, this requires a detailed understanding of the coordinated behavior of a very large number of interconnected metabolic reactions and metabolites. Toward this end, a systems biology approach, based on genome-scale metabolic models (GSMs) together with chemical structure-based toxicity target analyses, can be used to increase our understanding of toxicity mechanisms and help identify novel biomarkers associated with them.

GSMs represent the current knowledge of metabolism generated by integrating genetic and biochemical studies coupled with cellular, physiological, and clinical data and have emerged as a useful tool for the study of cellular metabolism (Nielsen 2009; Terzer et al. 2009; Gille et al. 2010; Thiele and Palsson 2010; Mardinoglu et al. 2013; Blais et al. 2017; Brunk et al. 2018; Wang et al. 2021). GSMs are composed of thousands of reactions and metabolites interconnected according to the stoichiometric matrix of the network. They also account for gene-protein-reaction (GPR) rules that map the relationship between genes, the proteins they encode, and the reactions they catalyze in the network. Therefore, these networks allow us to predict alterations in cellular metabolism based on changes in gene expression and can be applied to address questions related to toxicological studies (Carbonell et al. 2017; Brunk et al. 2018; Pannala et al. 2018). In our previous work, we developed rat GSMs and extensively used them to characterize the effects of several drug and environmental compounds on liver and kidney metabolism and identified potential metabolite biomarkers associated with their mechanism of toxicity (Blais et al. 2017; Pannala et al. 2019, 2020a, 2020b, 2020c; Rawls et al. 2021).

In this study, we leveraged the HTT data from rat 5-day dose-response studies performed by NTP using 18 different drugs or environmental chemicals (Gwinn et al. 2020) to understand and predict the alterations in liver metabolism due to toxicant exposure. We divided the chemical exposures into non-hepatotoxic and hepatotoxic based on the information from chronic liver toxicity studies (Gwinn et al. 2020) and obtained the derived whole transcriptomic data for these chemicals from our previous study (Pannala et al. 2023). We then used these derived whole gene expression profile data to explore how liver metabolic responses differed between the 2 classifications compared with their respective controls using chemical structure-based and rat GSM-based analyses.

First, using a chemical structure-based toxicity target profiler webtool (AbdulHameed et al. 2021), we identified the potential toxicity targets/molecular initiating events associated with the query chemicals. Many of the identified toxicity targets belong to various classes of transcriptional factors, and we created a list of downstream genes driven by them for all the chemicals used in the study. We then analyzed how mapping these genes onto the derived whole gene expression profiles obtained from the HTT platform can provide useful molecular signatures or mechanistic insights for depicting the predefined toxicity outcomes identified in the chronic studies. Our analysis of the changes in transcription factor-driven genes clearly indicated a distinct gene expression pattern for hepatotoxic chemicals compared with non-hepatotoxic chemicals, indicating their usefulness in classifying liver responses to toxicity. Second, we updated our previously developed rat GSM (Pannala et al. 2020c) by adding new biochemical reactions and correcting several reactions for stochiometric consistency based on the latest information from literature studies (Wang et al. 2021). Using this updated model, we integrated the derived whole gene expression profiles into the rat GSM and investigated whether the metabolic alterations predicted by the model can differentiate hepatotoxic exposures from non-hepatotoxic exposures. Our analysis revealed that the expression patterns of genes mapped to the metabolic model definitively showed an upregulated behavior both at the gene and pathway levels for hepatotoxic chemicals compared with non-hepatotoxic chemicals. Furthermore, our rat GSM-based approach was able to identify potential metabolites that changed differently between the 2 chemical classes in various cellular pathways, which can be studied in targeted assays to identify biomarkers for liver toxicity.

Materials and methods
Rationale for chemical selection

One of our primary goals in this study was to quantify the liver's responses upon exposure to hepatotoxic and non-hepatotoxic

chemicals. To achieve this goal, we relied on NTP 5-day rat studies where rats were exposed to a diverse set of environmental and drug-like chemicals that had their hepatotoxicity previously evaluated in repeated dosing studies (Gwinn et al. 2020). All of the chemicals we selected were tested in 90-day sub-chronic or 2-year chronic studies, except for fenofibrate. Furthermore, all the chemicals were orally administered, and the chemical-related increased incidences of liver histopathological effects were documented for a systemic comparison. Based on these histopathology outcomes, we broadly divided the chemicals into 2 major categories, i.e. non-hepatotoxic and hepatotoxic, which allowed us to simultaneously compare liver transcriptomic responses under similar conditions across all the chemicals in the current study.

Experimental dataset and derived whole transcriptomic data

We used experimental data from publicly available NTP 5-day in vivo rat studies that include the TempO-Seq HTT S1500+ dataset obtained from rats exposed to a diverse set of chemicals at different dose levels and the matched control groups (Gwinn et al. 2020). In these experiments, 8- to 10-week-old male Sprague Dawley rats were exposed to 8 or 9 concentrations of each of the 18 selected chemicals, along with a control group. Figure S1 shows all the chemicals, their dose levels, and their corresponding vehicle controls used in this study. The chemicals were administered via oral gavage (5 ml/kg) once per day for 5 consecutive days (Days 0–4), with 4 animals for each dose and a vehicle control ($n = 4$). On Day 5, the rats were exsanguinated and the liver tissues were collected for TempO-Seq-based HTT analysis (Gwinn et al. 2020). The normalized gene expression signals of the HTT S1500+ dataset, in terms of $\log_2$(counts per million+1) values, were then extrapolated to the whole rat transcriptome to obtain the derived whole gene expression profiles for all the samples, as described in our previous study (Pannala et al. 2023).

Differential gene expression and KEGG pathway enrichment analysis

Using the derived whole gene expression profiles for each dose and chemical together with their corresponding control samples from the HTT S1500+ dataset, we identified differentially expressed genes by performing a 1-way analysis of variance and estimated the false discovery rate (FDR) to correct for multiple comparisons. We defined a significantly expressed gene as one with an FDR-adjusted P-value <0.1. We used the resulting differentially expressed gene fold-change values for all of our subsequent analyses. For the KEGG pathway enrichment analysis, we used the aggregated fold-change (AFC) method, which provided directionality of gene expression in terms of whether the pathway was up- or downregulated (Yu et al. 2017). Briefly, using the differentially expressed gene fold-change values, the AFC method calculated the mean fold-change value for each gene and defined the KEGG pathway score as the total fold-change value of all the genes in the pathway. The sign of the pathway score represented the direction of regulation, with positive values indicating upregulation and negative values indicating downregulation in the treatment condition compared with their corresponding controls.

Chemical structure-based toxicity target profiler

We used the webtool ToxProfiler to obtain potential toxicity targets based on the structure of a chemical to predict the probability of its binding to an established toxicity target (AbdulHameed et al. 2021). We obtained the structures of the chemicals used in this study from the literature and used them as input to ToxProfiler (Table S1) (http://datadryad.org/stash/share/RM9HKUOf8PCb-STlufXehShPuXyTbRenn7i_Cl6bmIQ). Briefly, ToxProfiler uses a chemical structure-similarity-based read-across approach to generate a toxicity target profile for a query chemical based on several target representatives that are known to interact with the toxicity targets (64 toxicity targets). The webtool uses the 2D similarity approach to determine the similarity between the query molecule and the reference set of molecules. For each query compound, ToxProfiler displays the compound name, chemical structure, and a z-score-based toxicity target profile bar as output. The z-score values represent the level of similarity between the query compound and the target representatives. For example, z-score values greater than 1.960 indicate a high probability of interaction with the toxicity target, values less than 1.645 indicate no interaction, and values between the 2 extremes (1.645–1.960) indicate an uncertain prediction, with a potential for interaction of the query compound with the toxicity target.

We used the Transcriptional Regulatory Relationships Unraveled by Sentence-based Text mining (TRRUST) database (Han et al. 2018) to collect the genes that are driven by the toxicity targets identified using ToxProfiler. The TRRUST database is a curated repository of human and mouse transcription factors and target interactions and contains genes that act as transcription factors mapped to their target genes and the type of interaction (activation, repression, or unknown). Based on the human transcription factors and their regulatory interactions, we identified a list of transcription factors and their targeted genes and converted them into rat gene symbols using the online DAVID gene ID conversion tool (Huang et al. 2008).

Development of an updated rat GSM

We used the rat GSM iRno_ver3 (see Supplementary Models) (http://datadryad.org/stash/share/RM9HKUOf8PCb-STlufXehShPuXyTbRenn7i_Cl6bmIQ) that was previously developed by our group (Pannala et al. 2020c) and updated it with 2 crucial features: (i) we updated the model for stoichiometric consistency with respect to proton balance, and (ii) we added new reactions from a recently published rat network model, i.e. ratGEM (Wang et al. 2021). Briefly, to update iRno_ver3, we compared the reaction identifiers in the ratGEM model to determine which reactions were not present in iRno_ver3 based on the reaction mapping information provided in the ratGEM model (Table S2). The ratGEM model missed annotation for several reactions that are part of iRno_ver3 due to mismatches in the reaction identifier annotation or to various synonyms for the metabolites that are part of the reactions. We identified the reactions in iRno_ver3 that are part of the ratGEM model and included the respective reaction identifiers and corrected any mismatches with respect to metabolites and GPR associations (Table S3). This exercise allowed us to identify a set of provisional reactions that are unique to iRno_ver3 and not part of the ratGEM model.

To further differentiate reactions that are unique to each model, we compared both models using the name of the reaction, the name of the metabolites (and metabolite identifiers) that take part in the reaction, and the corresponding GPR associations together with the stoichiometry of the reaction under consideration. We note that our original rat GSM was built based on neutral formulas for the reaction metabolites, leading to several mismatches between the 2 models due to proton imbalance. Therefore, we first probed the iRno_ver3 model for charge

balance and updated all the reactions that had proton imbalance (Table S3) and provided charged formulas for all the metabolites in the updated model. Subsequently, our comparison yielded reactions that are unique to the ratGEM model, so we added them into our iRno_ver3 model (Table S3). To add these reactions, we converted all the metabolite and gene identifiers for each ratGEM reaction into the iRno_ver3 format and added a new metabolite if it did not exist already in the iRno_ver3 model. We performed all these operations using the COBRA Toolbox (version 3.1) for MATLAB (Heirendt et al. 2019) and named the updated rat GSM iRno_ver4. We provide our original model as well as the updated versions in SBML format as part of the Supplementary Models (http://datadryad.org/stash/share/RM9HKUOf8PCb-STIuf XehShPuXyTbRenn7i_Cl6bmIQ).

Algorithm for data integration and metabolite predictions

For the transcriptomics data integration, we used the transcriptionally inferred metabolic biomarker response (TIMBR) algorithm (Blais et al. 2017). Briefly, the TIMBR algorithm uses the GPR relationships in the model to convert the changes in gene expression (logarithmic fold-change values) into reaction weights. The algorithm first associates default weights with each reaction based on whether the reaction was a biochemical, transport, or boundary reaction. Next, it multiplies the gene expression value and the default value for reactions that have measured gene expression changes in the experimental data. Then, TIMBR calculates the global network demand required for producing a metabolite in the external serum compartment. Here, the objective function minimizes the weighted sum of fluxes across all reactions for each condition and metabolite to satisfy the associated mass balance and the optimal fraction of the maximum network capability to produce that metabolite. TIMBR calculates the raw production scores for each metabolite in the network for control and exposure conditions, translates these values to a z-score value, and represents them as a TIMBR z-score for each metabolite. The positive and negative values of the TIMBR z-scores indicate the propensity of a metabolite to be secreted (increased levels in serum compared with controls) and consumed (decreased levels in serum compared with controls), respectively (Pannala et al. 2018).

Results

Chemical structure-based analysis reveals gene expression patterns predictive of liver toxicity

In this study, we leveraged the HTT S1500+ platform-derived whole transcriptomic datasets, obtained from 5-day rat studies, to evaluate the predictive capability of changes in liver gene expression in response to chemical exposures. The study included a diverse set of drugs and environmental chemicals that were evaluated for their hepatotoxicity using chronic and sub-chronic studies (Gwinn et al. 2020). To understand the potential molecular initiating events by which these chemicals might initiate liver injury, we used a chemical-similarity approach (ToxProfiler) and evaluated whether the chemical has the potential to bind with any known toxicity targets (including transcription factors) based on their chemical structure (AbdulHameed et al. 2021). Figure 1 shows the ToxProfiler results for all 18 chemicals in a network diagram with chemical names as nodes and their potential toxicity targets shown as edges. The chemicals are further divided into non-hepatotoxic and hepatotoxic categories based on their prior evidence of hepatotoxicity. Our results

suggested a clear chemical-protein interaction (indicated with solid red line in Fig. 1) for several hepatotoxic chemicals that are predicted to interact with nuclear receptors (orange ovals). However, we observed that one of the non-hepatotoxic chemicals (TBBPA) was also predicted to interact with nuclear receptors, whereas 2 hepatotoxic chemicals (PUL and FUR) only showed a potential chemical-protein interaction with the nuclear receptor family (indicated with a yellow line in Fig. 1). We provide a complete list of toxicity targets in Table S4. At least 4 hepatotoxic chemicals were predicted to bind to toxicity targets of the androgen receptor (AR), estrogen receptors (ESR1 and ESR2), and peroxisome proliferator-activated receptors (PPARA and PPARD). These results suggest that the majority of the hepatotoxic chemicals bind with a family of nuclear receptors as molecular initiating events that drive the subsequent downstream alterations, which may lead to a toxic liver injury compared with non-hepatotoxic chemicals. These nuclear receptors act as transcription factors and modulate the expression of downstream genes.

To further understand the downstream alterations driven by the toxicity targets, we collected genes that are modulated by these potential molecular initiating events using the TRRUST database (Han et al. 2018). Overall, we identified 350 downstream genes that are driven by the known transcription factors or toxicity targets for which our ToxProfiler analysis showed a chemical-protein interaction (Fig. 1; Table S4). We were able to map ∼265 toxicity target-driven genes measured in our experimental data for each of the 18 chemicals. To understand the overall expression pattern of the mapped genes that indicate molecular initiation of toxicity-related processes, we looked at alterations in genes that are significantly modulated (FDR<0.1) at the highest dose of very toxic chemicals and monitored them at the highest dose across all the chemicals using hierarchical clustering. Figure 2A shows a clustergram plot of transcription factor-driven gene expression profiles at the highest dose of non-hepatotoxic (names in light gray on the x-axis) and hepatotoxic chemicals (names in dark gray on the x-axis), with their corresponding toxicity targets indicated on the y-axis. Our chemical-based clustering clearly separated the gene expression responses, with most of the non-hepatotoxic chemicals clustered together and away from hepatotoxic chemicals. Furthermore, the majority of the gene logarithmic fold-change values were downregulated (indicated in green) and not statistically significant for non-hepatotoxic chemicals, whereas they were upregulated (indicated in red) and statistically significant (FDR<0.1) across all the hepatotoxic chemicals at the highest dose. However, we did observe some exceptions. For example, MTE (non-hepatotoxic) and TCCP (hepatotoxic) showed opposite gene expression behavior compared with the other chemicals. Although most of the hepatotoxic chemicals induced an increase in the fold change of these genes, TCCP showed decreased fold-change values for the majority of the genes at the highest dose. Similarly, MTE showed increased gene fold-change values at the highest dose, whereas the other non-hepatotoxic chemicals showed decreased values. These results suggest multiple mechanisms that may lead to liver toxicity and require further in-depth studies on these individual chemicals to understand their mechanism of toxicity. We provide a complete list of all these genes together with their logarithmic fold-change values across all the dose conditions and chemicals in Table S5.

Figure 2B shows a violin plot of the distribution of logarithmic fold-change values for the toxicity target-driven genes, selected as in Fig. 2A, at the highest concentration across all the chemicals. The violin plots clearly show that the median value (the
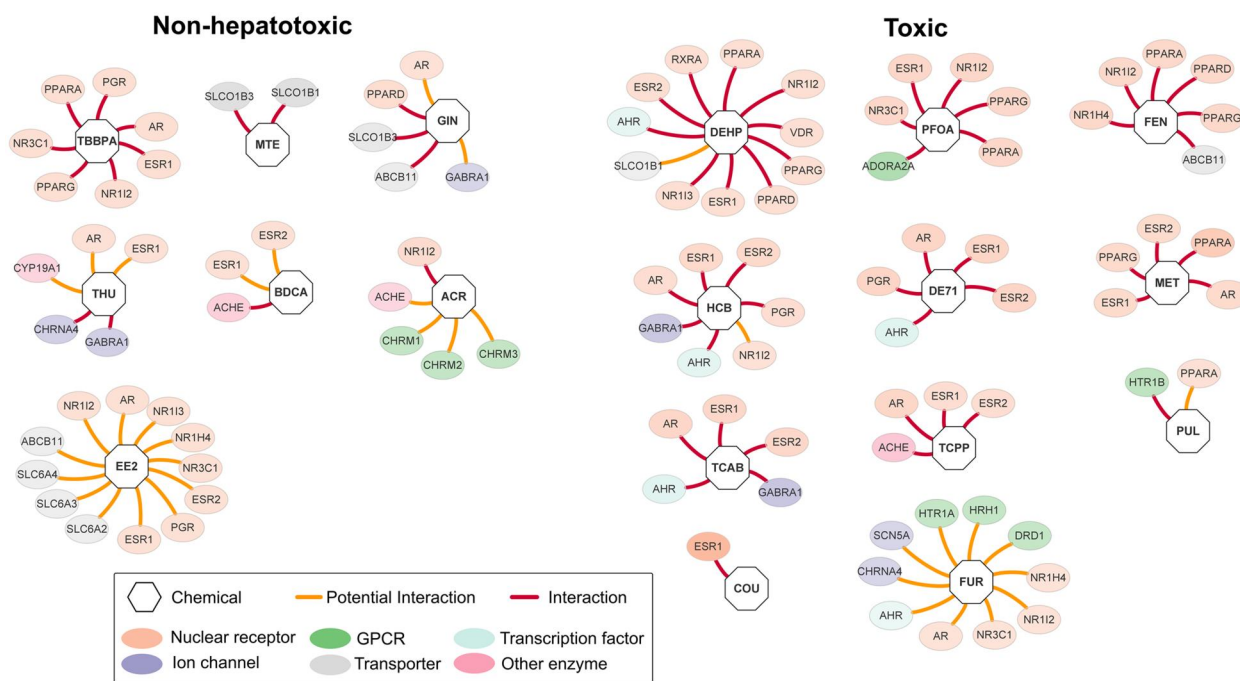
Fig. 1. Chemical structure-based prediction of toxicity target interaction profiles. ToxProfiler predictions for the set of 18 chemicals based on their structure as input (SMILES). Each octagon represents a chemical node, and each edge represents a toxicity target for the chemical. Nodes and edges connected by a solid red line denote a high probability of binding between the chemical and the toxicity target, and those connected by a yellow line indicate a potential interaction. GPCR, G protein-coupled receptor. See Table 1 for the definitions of the 18 chemicals and Table S4 for the complete list of toxicity targets and their downstream genes. (For interpretation of the references to color in this figure legend, the reader is referred to the web version of this article.)

white dot in the middle of the distribution) for the majority of the non-hepatotoxic chemicals was around zero. A very narrow distribution shape of the data for non-hepatotoxic chemicals GIN, BDCA, ACR, and THU indicates that the gene expression changes for these chemicals were negligible, indicating no major changes in the downstream genes that were driven by the known toxicity targets. However, the median of the gene fold-change values was slightly shifted to positive values for MTE ($\sim$0.11), indicating marginal perturbations in liver processes that are driven by the molecular initiating events for this chemical. We observed a similar behavior for the chemicals EE2 and TBBPA, with gene fold-change values indicating a negative shift in the median value around −0.13 and −0.19, respectively. In contrast, the median and interquartile range values for the hepatotoxic chemicals were shifted significantly toward positive values, except for TCPP, indicating a clear upregulated behavior. The chemical DE71 showed maximum perturbations with median logarithmic fold-change values around 0.68, followed by PUL, FUR, FEN, and PFOA with values of 0.54, 0.44, 0.4, and 0.38, respectively. These results show that for the majority of these hepatotoxic chemicals, the toxicity target-driven genes were significantly upregulated, leading to potential activation of several molecular initiating processes that are involved in liver toxicity.

An updated rat GSM to understand the mechanisms of liver toxicity

We expanded our previously developed rat GSM (iRno_ver3) by reviewing the literature for evidence of metabolic reactions we had not yet captured and adding new metabolites that participated in these reactions (Wang et al. 2021). We converted our model to include charge balance for all the metabolic reactions and included a new model field with charged formulas for all the metabolites. Overall, we corrected 2,099 reactions for charge

balance and added 4,486 new reactions with 2,669 metabolites (of which 933 are unique metabolites) into the updated rat GSM (Table S3). We corrected several anomalies: The metabolites phenylacetylglycine and chenodeoxycholic acid were duplicated, whereas several reactions existed as 2 unidirectional reactions, which we converted into a single bidirectional reaction for simplicity. Furthermore, based on the literature evidence, we also incorporated an additional compartment of inner mitochondrial space to accurately represent oxidative phosphorylation-related reactions. This curation effort resulted in a new rat GSM (iRno_ver4) with 13,043 reactions, 8,425 metabolites, and 3,102 unique genes (see Supplementary Models). The developed model successfully captured several previously defined liver-specific metabolic tasks, indicating the model's capability to simulate liver metabolism (Blais et al. 2017). We used this model in our subsequent analyses to understand the liver metabolic responses by integrating gene expression data from rats exposed to different drugs and environmental chemicals.

Metabolic genes show distinct expression patterns across hepatotoxic chemicals compared with non-hepatotoxic chemicals

The S1500+ platform-derived gene expression profiles for each chemical contain thousands of genes and provide certain expression features that provide useful information regarding liver toxicity. However, the rat GSM provides an opportunity to understand the liver responses specifically through the lenses of metabolic reactions that drive liver metabolism. Therefore, we mapped the genes identified in the expression data for all chemicals onto the rat GSM, which contains 3,102 unique metabolic genes, and looked at how the expression pattern of these mapped genes differed between non-hepatotoxic and hepatotoxic chemicals. Figure 3A shows a hierarchical clustering plot of logarithmic
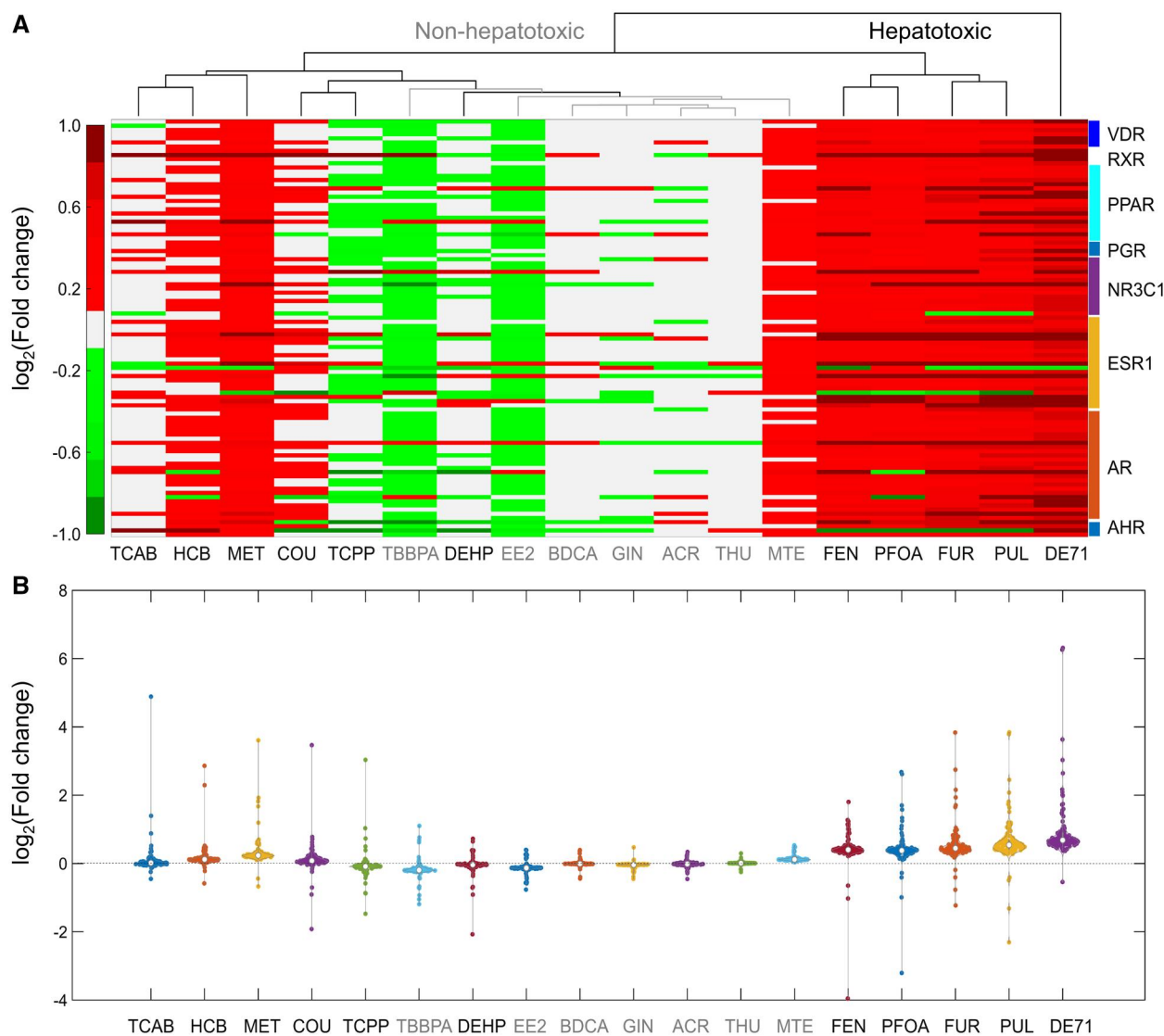
Fig. 2. Alterations in the toxicity target regulated downstream genes that changed significantly (false discovery rate<0.1) at the highest concentration of very toxic chemicals and monitored across all 18 chemicals at the highest concentration. (A) Hierarchical clustering of the logarithmic fold-change values of genes driven by toxicity targets (labels on the y-axis) at the highest dose based on row-wise clustering across the chemicals. Red and green indicate genes that were up- and downregulated, respectively. (B) A violin plot of the distribution of logarithmic gene fold-change values for the toxicity target regulated downstream genes for hepatotoxic (chemical names in black) and non-hepatotoxic chemicals (chemical names in light grey). AHR, aryl hydrocarbon receptor; AR, androgen receptor; ESR1, estrogen receptor 1; NR3C1, glucocorticoid receptor; PGR, progesterone receptor; PPAR, peroxisome proliferator-activated receptors; RXR, retinoid X receptor; VDR, vitamin D receptor. (For interpretation of the references to color in this figure legend, the reader is referred to the web version of this article.)

fold-change values of mapped genes that are common at the highest dose of very toxic chemicals and monitored at the highest dose across all chemicals. We observed a clear separation of hepatotoxic chemical responses in our hierarchical clustering, with the majority of the hepatotoxic chemicals clustered together, except DEHP and TCCP, which were clustered close to the non-hepatotoxic chemicals. We observed a clear trend in that the majority of the genes were downregulated (indicated in green) and not statistically significant for most of the non-hepatotoxic chemicals (GIN, BDCA, ACR, and THU) at the highest dose level. We observed a similar trend for hepatotoxic chemicals at the lower concentrations, however, the trend was reversed as concentration increased and the majority of the genes were upregulated at the highest dose, indicating potential toxicant-mediated responses that may lead to liver toxicity. We could see this behavior more clearly in violin plots at the highest dose of each chemical, as shown in Fig. 3B. The median values of the distribution of logarithmic fold-

change values were much higher for hepatotoxic versus non-hepatotoxic chemicals, indicating hepatotoxicant-specific metabolic responses in the liver. We provide a complete list of all the model-mapped genes together with their logarithmic fold-change values across all dose conditions and chemicals in Table S6.

To further understand the biological significance of changes in these mapped metabolic genes at the pathway level, we performed a KEGG pathway enrichment analysis using the genes mapped to the metabolic model. Table 1 shows a summary of the number of significantly differentially expressed genes (FDR<0.1) at the highest concentration or the concentration at which the maximum perturbations were observed for each chemical and how many of these genes were mapped to the rat GSM. We did not find many significant genes for 4 non-hepatotoxic chemicals (THU, ACR, EE2, and BDCA), so we omitted them from our KEGG pathway enrichment analysis. Figure 4 shows the significantly
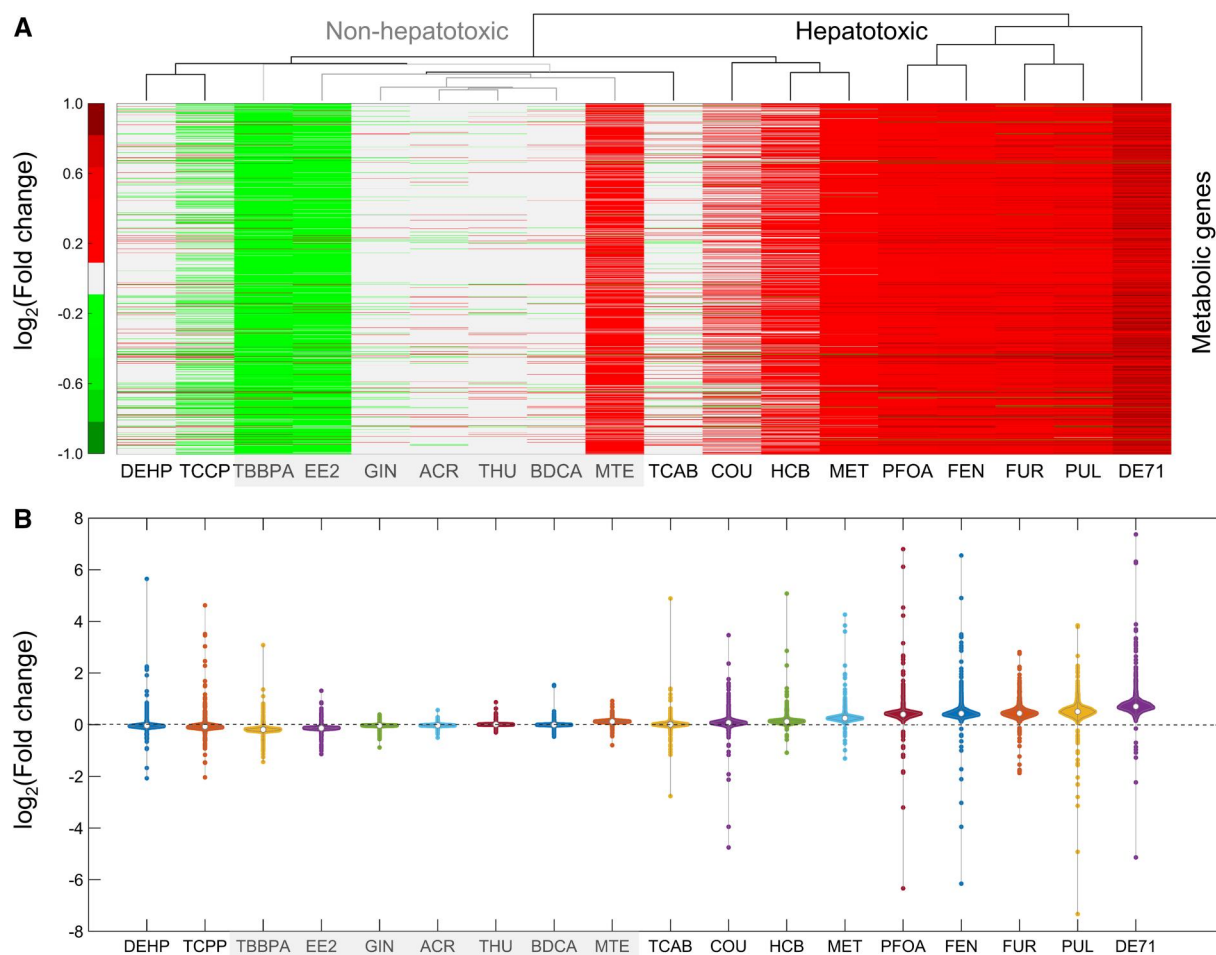
Fig. 3. Alterations in the rat genome-scale metabolic model (GSM) mapped metabolic genes that changed significantly (false discovery rate<0.1) at the highest concentration of very toxic chemicals and monitored across all 18 chemicals (see Table 1) at the highest concentration. (A) Hierarchical clustering of logarithmic fold-change values of genes that are common for all the chemicals at the highest dose and clustered based on rows. Red and green indicate genes that were up- and downregulated, respectively. (B) A violin plot of the distribution of gene fold-change values for the rat GSM mapped genes at the highest concentration of non-hepatotoxic (chemical names in light grey) and hepatotoxic chemicals (chemical names in black). (For interpretation of the references to color in this figure legend, the reader is referred to the web version of this article.)

altered metabolic pathways for the rest of the chemicals at the highest dose or at the maximum gene perturbations as pathway AFC z-score values. The colors indicate if the metabolic pathways were either upregulated (red) or downregulated (green) compared with their control conditions. We observed a distinct pathway alteration behavior as several metabolic pathways were upregulated for hepatotoxic versus non-hepatotoxic chemicals. Specifically, most of the hepatotoxic chemicals showed commonalities in the upregulation of pentose and glucuronate interconversion, ascorbate and aldarate, steroid hormone biosynthesis, fatty acid, arachidonate, linoleic acid, alpha-linolenic, glutathione, retinol, and drug metabolism-related pathways. We also observed several pathway alterations that are common for the chemicals FEN and PFOA as a pair and FUR and PUL as another pair. Interestingly, the non-hepatotoxic chemical TBBPA showed many pathway alterations that are similar to the hepatotoxic chemicals at the highest concentration, indicating its potential for hepatotoxicity.

Rat GSM predicts changes in serum metabolite levels using gene expression data

To obtain the alterations in liver metabolism due to toxic chemical exposures at the metabolite level, we used our updated rat

GSM (iRno_ver4) together with the derived gene expression data from HTT S1500+ studies and applied the TIMBR algorithm to determine the capability of the rat GSM to predict whether each metabolite would be produced or consumed in the serum. Here, we used all the genes that are mapped to the model, irrespective of whether the gene fold change was statistically significant, to make a prediction. Overall, we were able to make TIMBR predictions for 1,090 metabolites based on differentially expressed genes for each chemical and dose condition. Figure 5A shows a hierarchical clustering of all the predicted metabolites at the lowest dose across all the non-hepatotoxic chemicals compared with the highest dose for the hepatotoxic chemicals. The hierarchical clustering, based on metabolite z-score values, followed a similar hierarchy that we observed with respect to alterations in metabolic genes in Fig. 3A and clearly separated hepatotoxic chemicals from non-hepatotoxic chemicals, with all the non-hepatotoxic chemicals at the highest dose level clustered away from the hepatotoxic chemicals. We identified a distinct set of clustered metabolites for which the model predicted reduced TIMBR z-scores, indicating the metabolite was consumed (shown in green), for the non-hepatotoxic chemicals but increased z-scores, indicating production (shown in red), for the hepatotoxic

Table 1. Summary of the number of significantly differentially expressed genes (FDR<0.1) at the highest concentration or the concentration at which maximum gene perturbations were observed for each chemical and the number of genes that were mapped to the rat genome-scale metabolic model.

Chemical	Total genes	DEGs (FDR<0.1)	Genes mapped to iRno_ver4	Mapped DEGs (FDR<0.1)
Milk thistle extract (MTE)	11,800	8,646	2,341	1,643
Ginseng (GIN)	11,964	8,200[a]	2,364	1,681
Bromodichloroacetic acid (BDCA)	11,783	6	2,344	3
Acrylamide (ACR)	11,972	0	2,364	0
α,β-Thujone (THU)	12,028	1	2,370	1
Ethinyl estradiol (EE2)	11,867	87	2,355	36
Tetrabromobisphenol A (TBBPA)	12,228	11,222[a]	2,395	2,135
Di(2-ethylhexyl)phthalate (DEHP)	11,756	163	2,346	83
Coumarin (COU)	12,035	1,059	2,373	271
Pentabromodiphenyl ether mixture (DE71)	11,364	10,596	2,308	2,095
3,3′,4,4′-Tetrachloroazobenzene (TCAB)	11,880	219	2,354	61
Hexachlorobenzene (HCB)	11,794	4,272	2,348	693
Methyl eugenol (MET)	11,932	10,457	2,355	2,024
Tris(chloropropyl)phosphate (TCPP)	11,796	9,203	2,352	1,780
Fenofibrate (FEN)	11,650	10,376	2,326	2,033
Perfluorooctanoic acid (PFOA)	11,557	10,330	2,323	2,036
Furan (FUR)	11,993	10,702	2,368	2,002
Pulegone (PUL)	11,735	10,387	2,340	1,908

Names in normal and bold font indicate the chemicals classified as non-hepatotoxic and hepatotoxic, respectively. DEGs, differentially expressed genes; FDR, false discovery rate.
[a] Maximum DEGs observed at an intermediate dose.

Pathway	MTE	GIN	TBBPA	DEHP	COU	DE71	TCAB	HCB	MET	TCPP	FEN	PFOA	FUR	PUL
						AFC z-score								
Pentose and glucuronate interconversions	1.82	-2.73	5.53	0.05	2.04	3.47	0.77	4.66	5.38	5.75	-0.18	2.10	3.36	-0.50
Ascorbate and aldarate metabolism	1.77	-2.77	7.90	0.02	1.72	1.77	0.77	4.98	4.74	8.29	-0.40	2.39	0.66	-3.88
Butanoate metabolism	0.36	-4.12	-0.82	2.10	-0.48	-1.99	-1.41	-1.58	-0.96	3.54	2.24	1.23	-4.29	-5.40
Fatty acid elongation	1.41	-0.97	-0.80	3.13	2.23	-0.02	-1.10	-0.46	0.12	1.17	8.92	8.60	2.11	-0.58
Fatty acid degradation	2.59	-3.31	-3.24	2.37	0.72	1.56	-1.41	-2.20	1.42	4.53	11.16	10.18	-0.69	-3.73
Steroid biosynthesis	3.28	-0.49	-1.44		1.74	-0.30		-0.25	1.80	0.44	-3.92	-2.91	1.48	
Steroid hormone biosynthesis	5.44	-6.76	7.87	-0.49	-1.16	10.16	3.87	11.02	7.97	7.95	-1.02	3.13	-6.22	-7.98
Fatty acid metabolism	3.63	-1.87	-2.81	2.88	1.16	1.57	-1.41	-1.27	1.19	2.26	9.65	7.57	-0.47	-1.51
Biosynthesis of unsaturated fatty acids	1.11	-0.91	-2.04	3.87	1.57	0.89	-1.10	-0.51	0.90	0.24	12.36	10.55	1.08	-1.15
Arachidonic acid metabolism	2.85	-4.06	1.53	0.20	-1.89	3.62	-0.39	3.45	4.50	1.52	0.77	2.08	-1.48	-0.80
Linoleic acid metabolism	2.12	-3.46	2.11	-1.56	-4.71	4.33	2.80	4.71	2.19	2.15	-3.89	-0.53	-7.31	-7.58
alpha-Linolenic acid metabolism	-0.23	-0.24	-1.16	1.93	1.76	0.92		-0.32	1.63	2.54	5.23	4.38	-0.10	1.45
Valine, leucine and isoleucine degradation	2.45	-3.40	-3.48	2.35	1.63	0.96	-1.41	-1.04	0.88	4.00	5.74	4.90	-1.12	-2.08
Tryptophan metabolism	-1.15	-1.46	-1.68	-0.38	-1.89	3.55	3.79	0.80	-1.00	1.68	1.44	0.12	-2.37	-4.93
Glutathione metabolism	2.47	-5.25	-1.60		3.04	7.03	0.96	4.00	7.13	-1.65	-0.71	-0.23	2.94	1.50
Retinol metabolism	1.18	-4.29	7.27	-0.35	-1.33	9.40	2.99	9.89	7.60	8.82	-1.02	4.36	-6.43	-8.54
Porphyrin and chlorophyll metabolism	-0.14	-0.61	2.86	0.05	1.92	4.58	0.77	5.51	2.83	4.33	0.39	1.82	-0.62	-0.20
Metabolism of xenobiotics by cytochrome P450	2.75	-4.96	3.04	-0.68	3.38	12.53	4.31	9.29	11.33	3.22	-1.66	0.93	1.22	-2.29
Drug metabolism - cytochrome P450	3.07	-3.56	5.13	-0.72	2.48	6.85	2.30	6.96	7.60	3.10	-2.69	0.13	-0.99	-4.47
Drug metabolism - other enzymes	1.22	-2.41	3.86	-0.54	3.16	6.02	1.40	4.70	5.26	3.31	-1.41	1.05	0.42	-1.99
Caffeine metabolism	-0.18	2.51	-2.53	-2.53	-1.20	3.73	2.80	5.73	-1.05	-2.82	-5.15	-3.62	-2.36	-3.71
PPAR signaling pathway	2.56	-6.06	-2.91	2.09	-0.65	0.22	-0.70	-0.65	1.38	-2.63	11.38	8.04	0.88	-3.85
Peroxisome	-1.05	-0.68	-2.96	1.46	-0.50	0.19	-1.71	-0.58	0.19	2.49	6.68	7.19	-2.38	-6.55
Serotonergic synapse	-0.12	-3.54	2.52	-0.79	-3.99	-0.59	-0.07	1.92	-0.17	2.01	-3.23	-0.57	-4.56	-4.66
Pathways in cancer	0.81	-1.05	-1.76		3.19	4.96	1.62	4.41	5.02	-0.46	-1.42	-0.82	1.62	1.79
Chemical carcinogenesis	2.47	-4.78	5.58	-0.46	0.88	13.17	4.23	12.45	10.86	6.56	-2.57	2.68	-4.25	-5.89
MicroRNAs in cancer	1.90	0.65	-1.49		1.71	3.92	2.60	-0.24	5.20	-0.33	0.01	-0.40	5.35	5.04
Fluid shear stress and atherosclerosis	0.89	-0.95	-2.50	-1.78	2.69	7.22	1.80	5.30	5.51	-1.93	-1.63	-1.84	1.67	1.29

Fig. 4. Summary of significantly altered metabolic pathways based on genes mapped to rat genome-scale metabolic model (GSM). An aggregated fold-change (AFC)-based z-score value was calculated for each pathway based on significantly altered genes (false discovery rate<0.1) mapped to rat GSM for each chemical at the highest dose (see Table 1). Red and green indicate significantly up- and downregulated metabolic pathways, respectively. (For interpretation of the references to color in this figure legend, the reader is referred to the web version of this article.)

chemicals compared with their control conditions (Cluster 1). Similarly, we identified that a large portion of the metabolites (Cluster 2) showed the opposite behavior, with a majority of the TIMBR z-scores increasing for non-hepatotoxic compared with hepatotoxic chemicals.

To quantify the extent of similarity between the predicted responses, we calculated the pairwise Pearson's correlation coefficients of the TIMBR z-scores for the lowest concentrations of non-hepatotoxic chemicals compared with the highest concentrations of hepatotoxic chemicals as shown in Fig. 5B. As expected, we observed a very good correlation between metabolites predicted for the hepatotoxic chemicals and a negative correlation for the non-hepatotoxic chemicals. We observed a similar behavior when we looked at the distribution of TIMBR z-scores for each chemical at the highest dose (Fig. S2). For the hepatotoxic chemicals, the violin plots clearly show that the TIMBR
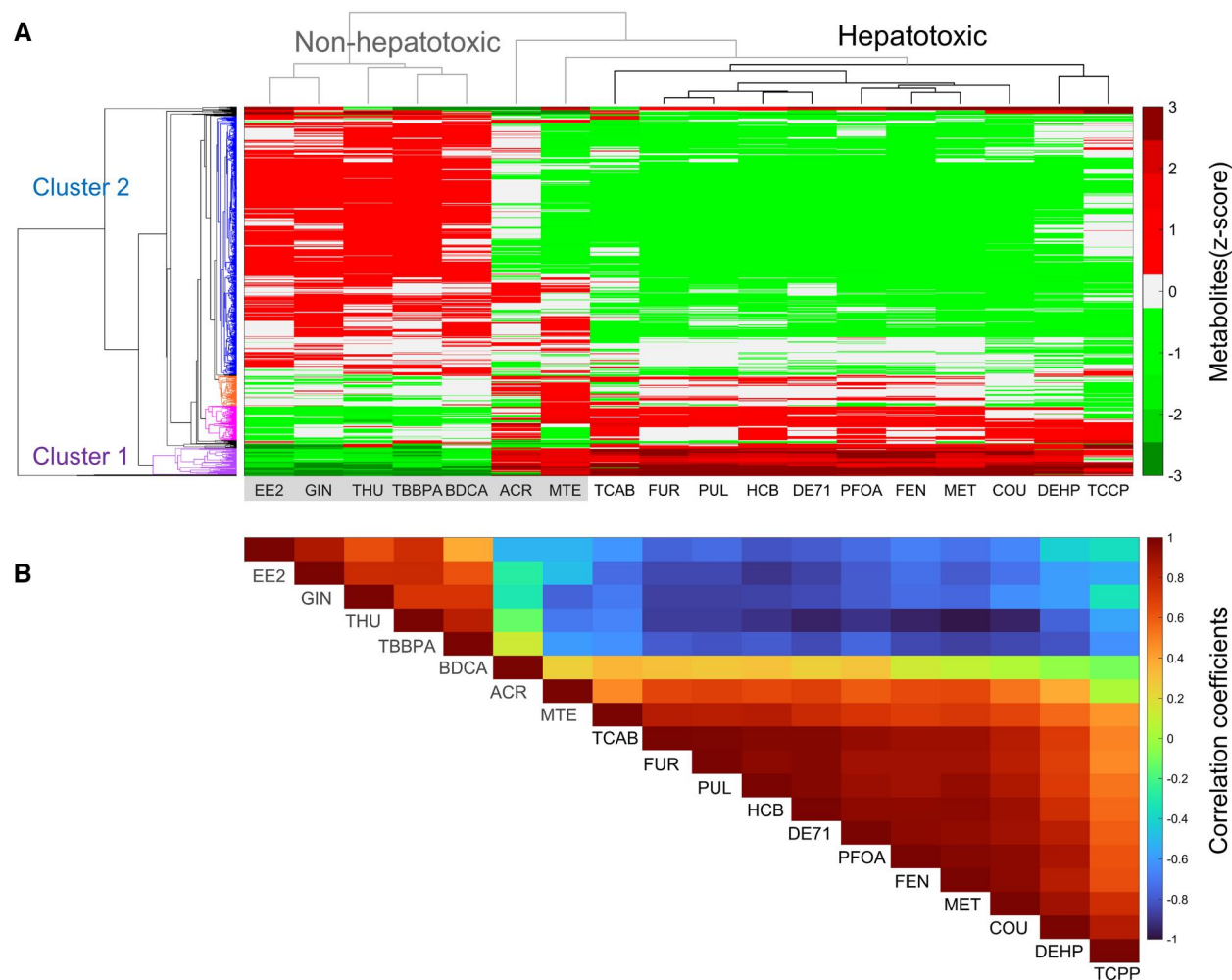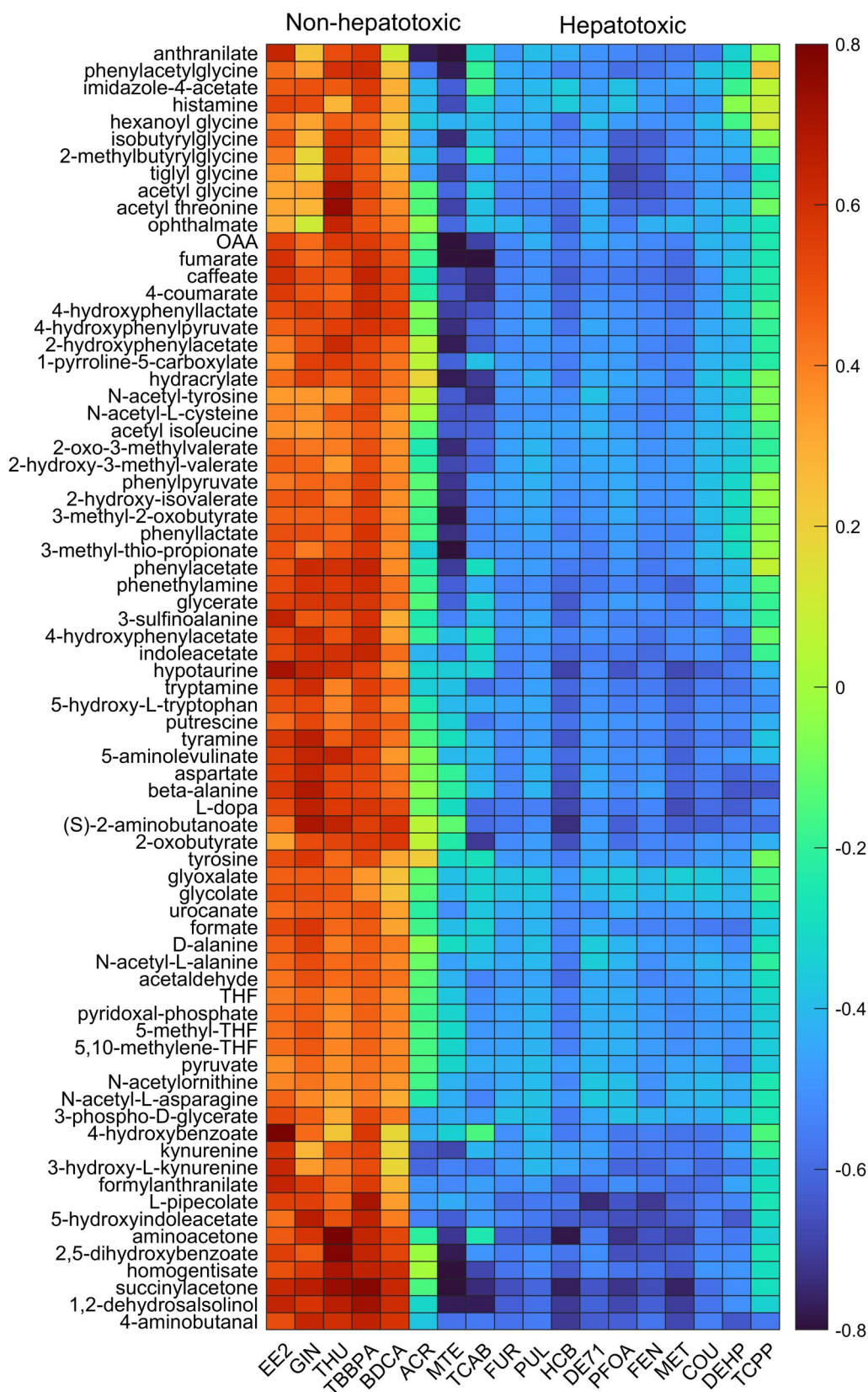
Fig. 5. Rat genome-scale metabolic model (GSM) predictions of serum metabolite levels based on gene expression changes in rat metabolism caused by exposure to the lowest dose levels across the non-hepatotoxic chemicals and to the highest dose level for the hepatotoxic chemicals. (A) Hierarchical clustering of transcriptionally inferred metabolic biomarker response (TIMBR) z-score values that are common for all 18 chemicals and clustered by both rows (genes) and columns (chemicals). Red and green indicate metabolites that were increased or decreased in serum compared with the control groups, respectively. (B) Pairwise Pearson's correlation coefficients for the altered metabolites at the lowest dose levels across the non-hepatotoxic chemicals and at the highest dose level for the hepatotoxic chemicals. (For interpretation of the references to color in this figure legend, the reader is referred to the web version of this article.)

z-scores decreased for the majority of the metabolites, with their median values well below zero, and increased for only a few metabolites. We provide a complete list of predicted metabolites together with their TIMBR z-scores in Table S7.

We next looked at how metabolites in the individual pathways were altered due to toxic chemical exposures. Since each reaction in the rat GSM is classified to one of the subsystems at the pathway level, we identified a list of metabolites that participate in different metabolic pathways, such as amino acid and lipid metabolism, and compiled the TIMBR z-scores for this set of metabolites. Figure 6 shows the hierarchical clustering of TIMBR z-scores for some of the metabolites at the lowest dose for non-hepatotoxic chemicals compared with the highest dose for hepatotoxic chemicals that participate in amino acid metabolism. Interestingly, for most of the amino acid-related metabolites, we found that their TIMBR z-scores were decreased for hepatotoxic chemicals, indicating their consumption due to toxicant exposure, whereas they were increased or unchanged for non-hepatotoxic chemicals. In addition, our analysis also indicated a dose-dependent response, with several of these metabolites

initially produced at the lower concentrations but consumed as the concentration increased for the hepatotoxic chemicals (Table S7).

Similarly, Figure 7 shows the hierarchical clustering of TIMBR z-scores for some of the metabolites at the lowest dose for non-hepatotoxic chemicals compared with the highest dose for hepatotoxic chemicals that participate in lipid metabolism (see Table S7 for the full list). Unlike the changes observed for amino acid metabolism, we found several distinct sets of metabolite clusters for lipid metabolism. We were able to identify a set of metabolites with an increase in TIMBR z-scores, indicating increased production in response to toxicant exposures for hepatotoxic chemicals, and their response was dose-dependent with a higher metabolite production probability at higher toxicant concentrations (Fig. 7). We also identified another set of metabolites with decreased TIMBR z-scores, indicating their consumption for hepatotoxic compared with non-toxic chemicals (Table S7). In addition, we observed a similar behavior in several metabolites involved in the carbohydrate and nucleotide metabolism pathways. Overall, these results indicate that the rat GSM can serve
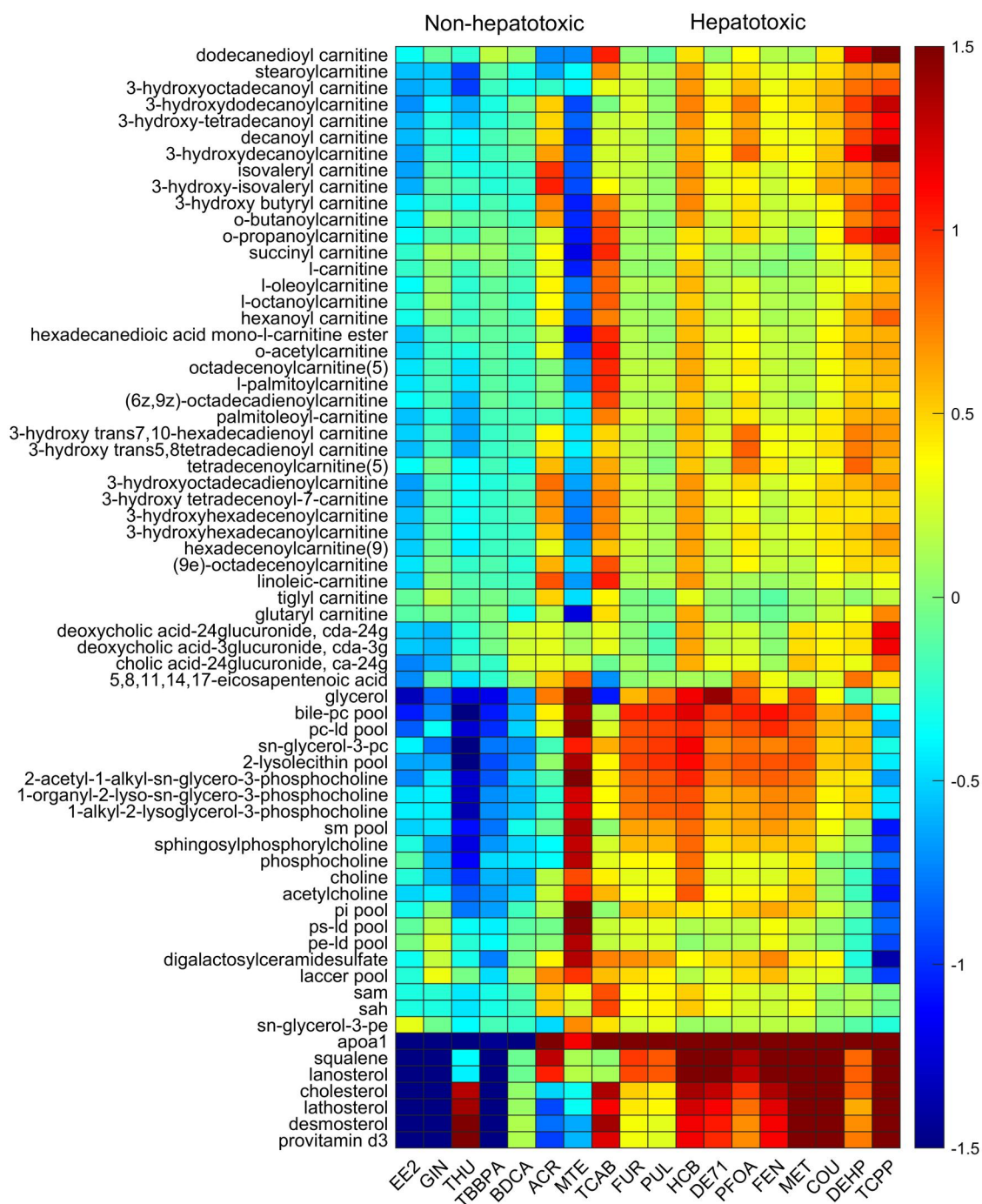
Fig. 6. Heatmap of amino acid metabolism-related metabolites. Rat genome-scale metabolic model (GSM)-based predictions of serum metabolite levels (z-score values) that are part of amino acid metabolism compared at the lowest dose levels across the non-hepatotoxic chemicals and the highest dose level for the hepatotoxic chemicals. Red and green indicate metabolites that were increased or decreased in the serum compared with the control groups, respectively. (For interpretation of the references to color in this figure legend, the reader is referred to the web version of this article.)

Fig. 7. Heatmap of lipid metabolism-related metabolites. Rat genome-scale metabolic model (GSM)-based predictions of serum metabolite levels (z-score values) that are part of lipid metabolism compared at the lowest dose levels across the non-hepatotoxic chemicals and the highest dose level for the hepatotoxic chemicals. Red and green indicate metabolites that were increased or decreased in the serum compared with the control groups, respectively. (For interpretation of the references to color in this figure legend, the reader is referred to the web version of this article.)

as a computational platform to identify specific sets of metabolites that are driven by gene expression changes and can be used to differentiate liver-toxic from non-toxic chemical exposures.

Discussion

HTT technologies currently enable us to simultaneously measure thousands of different genes in a traditional RNA-seq analysis or allow us to measure a short list of curated sets of genes (HTT S1500+) for different chemicals across multiple exposures to capture changes at the whole genome level (Gwinn et al. 2020). Although such gene lists provide valuable information regarding alterations across different phenotypes and play an important role in the downstream analysis, they alone cannot elucidate the complex mechanisms involved in the perturbations. Toward this end, to gain insights into the underlying mechanisms of liver toxicity induced by various drugs and environmental chemicals, we used HTT S1500+ platform-derived whole-genome gene expression changes for different chemicals across multiple conditions studied during a 5-day rat in vivo protocol (Gwinn et al. 2020).

The use of similar experimental conditions for all the chemical exposures and their separation into non-hepatotoxic and hepatotoxic chemicals allowed us to analyze them together and differentiate the non-toxic from the toxic liver responses. We used a chemical structure-based toxicity target analysis and identified potential toxicity targets in the liver and the corresponding downstream genes that elucidate the mechanisms behind the liver responses. Furthermore, we used GSMs, which enabled us to interpret systemic effects, understand the genotype-to-phenotype relationships for injury-specific pathways, and identify the associated metabolite alterations in the serum that can differentiate toxic from non-toxic liver responses.

When the liver is exposed to xenobiotics, it undergoes adaptive responses due to induction of hepatocellular drug metabolism following activation of nuclear receptors (Maronpot et al. 2010). For example, the adaptive responses include regulation of gene transcription by the constitutive androstane receptor (CAR), the pregnane-X-receptor (PXR), PPARA, or the aryl hydrocarbon receptor (AHR) (Mackowiak et al. 2018). These receptors drive several downstream genes, including phase I drug-metabolizing enzymes, and the intermediate free radical molecules produced during this process can cause oxidative stress to hepatocytes, leading in extreme cases to cell death. However, more subtle manifestations of toxicity often include alterations in crucial metabolic pathways, such as fatty acid synthesis and degradation or disruption of bile acid synthesis and excretion, that may result in several liver disease endpoints like steatosis, cirrhosis, cholestasis, and cancer (Padda et al. 2011; Basaranoglu et al. 2013; Leung and Nieto 2013).

Our chemical structure-based toxicity target analysis predicted that most of the hepatotoxic chemicals used in our study interact with nuclear receptors (Fig. 1). Nuclear receptors govern the expression of numerous genes involved in a wide range of cellular processes, including cell growth, differentiation, metabolism, and stress response. Our results show that out of the 11 diverse hepatotoxic chemicals used in this study, 6 chemicals (DEHP, DE71, TCAB, HCB, FEN, and PFOA) bind to at least one of the nuclear receptors (farnesoid X receptor, PXR, CAR, and AHR) that control the xenobiotic metabolizing enzymes. In addition, most of these chemicals (DEHP, DE71, TCAB, and HCB), along with TBBPA, were predicted to interact with AR and ESRs, indicating multiple mechanisms through which these chemicals may cause liver toxicity. Indeed, in several studies, AR and ESRs have been implicated in the development of chemical-induced hepatocellular carcinoma (Beck et al. 2016; Kharlyngdoh et al. 2018; Liu et al. 2021; Chen et al. 2022). Interestingly, we did not find AR and ESR interaction for the chemicals FEN, FUR, and PUL, however, FEN along with PFOA and MET were predicted to interact with PPAR receptors, indicating that the well-known PPAR signaling pathway is a potential mechanism associated with either adaptive or liver toxicity for these chemicals. Furthermore, we found that a substantial number of downstream genes associated with many of these transcription factors show a tendency for upregulation with different hepatotoxic chemicals, and many of them show a dose-dependent behavior (Fig. 2), which indicates that they should be tested further to identify them as robust markers for the liver toxicity.

To further understand the mechanisms through which these chemicals induce liver toxicity, we employed GSMs. These models allow us to pinpoint the genes or proteins of interest that are associated with an observed phenotypic response or to characterize the overall response to an altered state of the system. As part of this study, we first developed an updated rat GSM and validated its potential to simulate several liver metabolic functionalities. The developed model allowed us to identify various metabolic genes and pathways in rat metabolism that are specifically associated with liver metabolism (Figs. 3 and 4). Interestingly, a majority of these metabolic genes showed a dose-dependent upregulation behavior for most of the hepatotoxic chemicals, indicating their potential for use in differentiating toxic from non-hepatotoxic chemical exposures. A further pathway-level examination of the significantly altered genes (Table 1) indicated that hepatotoxic chemicals modified various pathways in carbohydrate, lipid, and amino acid metabolism. Specifically, we observed significant upregulations in steroid hormone biosynthesis, fatty acid, arachidonate, and linoleic acid metabolism across several hepatotoxic chemicals, indicating disruptions in lipid metabolism. Furthermore, we observed a significant upregulation in glutathione metabolism, indicating oxidative stress (Fig. 4). Interestingly, the observed alterations in the metabolic pathways qualitatively mimicked the results of our chemical structure-based toxicity target analysis results, with a majority of the hepatotoxic chemicals showing similarities in terms of their pathway alterations for certain groups of chemicals. For example, we observed several pathway commonalities for the chemicals DEHP, COU, DE71, TCAB, HCB, MET, and FEN. Similarly, we observed several pathway commonalities for the chemicals FEN and PFOA as they were predicted to interact with common toxicity targets. These results further strengthen our study and highlight the ability to use a combined approach to analyze the mechanisms behind liver toxicity.

Use of GSMs provides additional advantages as they link changes in gene expression with the phenotypic changes in terms of changes in metabolite levels in the serum, which can be detected non-invasively as markers for toxicity. Therefore, we integrated the gene expression changes across the 18 chemicals from the liver tissue to predict metabolite alterations in the serum. Overall, our results showed a dose-dependent reduction in a majority of the metabolites in the serum for hepatotoxic chemicals compared with non-hepatotoxic chemicals. Indeed, we observed a strong positive correlation for the hepatotoxic chemicals at the highest exposure levels and a negative correlation for the non-hepatotoxic chemicals (Fig. 5). Interestingly, as an indication of oxidative stress due to toxic chemical exposures, several amino acid-related metabolites were predicted to be consumed from the serum, and some of them were precursors to glutathione synthesis, one of the clearance mechanisms for toxic chemical exposures in the liver (Fig. 6). Furthermore, we identified several clusters of lipid-related metabolites that are dose-dependently either decreased or increased for only hepatotoxic chemicals, indicating toxic exposure-mediated lipid alterations. Therefore, our framework provides a mechanistic way to select a set of metabolites that are common to different hepatotoxic chemicals and can be utilized in a targeted analysis to determine their potential as biomarkers to predict liver toxicity.

Although the GSM approach provided a gene expression-based prediction of changes in metabolite uptake and secretion, we were not able to validate these predictions due to the absence of serum metabolite measurements for any of the chemicals under similar conditions. Furthermore, our prior experience with validation of GSM model predictions indicated that these changes may not be directly comparable with changes in serum metabolite concentrations due to lack of clarity in the GSM model's capability to differentiate tissue metabolites from the serum. Although these predictions represent data-driven hypotheses, there are multiple factors that need to be considered when

testing these predictions in biofluids, like urine and blood. One limitation of the current study is that we only consider expression data from liver tissue as the input under a given physiological nutrient uptake rate derived from literature studies to predict the probability of a metabolite being secreted or taken up by the liver from the serum. Alterations or variations in nutrient-uptake conditions and uptake/secretion from other organs can also affect the systemic circulation of metabolites in biofluids. Furthermore, our previous GSM studies indicated that gene expression changes alone are insufficient to fully account for metabolite plasma-level changes and suggest additional regulatory factors, such as posttranslational modification, gene regulation, and metabolite feedback, that ultimately result in the observed serum metabolite levels (Pannala et al. 2018). Therefore, comparison of TIMBR z-scores with serum metabolite concentrations should be interpreted cautiously. Future studies that utilize datasets with paired multi-omics datasets to constrain and validate modeling results can provide a more precise hypothesis-generating capability.

In summary, we utilized a combined chemical structure-based and systems biology approach to probe alterations in liver metabolism that are common to different liver-toxic chemicals and identified a targeted set of genes as well as global changes in serum metabolite levels. We identified significant commonalities across hepatotoxic chemicals reflecting their mechanisms of toxicity and observed dose-dependent alterations that are maximally correlated at their peak concentration levels. Furthermore, we developed the latest version of the rat GSM, and using these models, we identified several injury-specific pathways that are related to amino acid and lipid metabolism and identified several metabolites in serum that are predicted to be significantly altered due to toxic chemical exposures. Our results using this rat GSM-based approach showed good agreement with the chemical structure-based toxicity analysis, indicating its potential to serve as a useful tool to integrate high-throughput data from multiple toxicants, elucidate the underlying mechanism of toxicity, and provide ways to differentiate toxic from non-toxic chemicals.

Acknowledgments

Author contributions

Conceptualization: Venkat R. Pannala and Anders Wallqvist; methodology and analysis: Venkat R. Pannala, Archana Hari, and Mohamed Diwan M. AbdulHameed; data curation, processing, and quality control: Michele R. Balik-Meisner, Deepak Mav, Dhiral P. Phadke, Elizabeth H. Scholl, Ruchir R. Shah, and Scott S. Auerbach; writing—original draft preparation: Venkat R. Pannala; writing—review and editing: Venkat R. Pannala, Archana Hari, Mohamed Diwan M. AbdulHameed, Michele R. Balik-Meisner, Deepak Mav, Dhiral P. Phadke, Elizabeth H. Scholl, Ruchir R. Shah, Scott S. Auerbach, and Anders Wallqvist; supervision: Anders Wallqvist; funding acquisition: Anders Wallqvist. All authors have read and agreed to the published version of the manuscript.

Supplementary material

Supplementary material is available at *Toxicological Sciences* online.

Funding

Conflicts of interest

None declared.

Data availability

The datasets presented in this study are derived from the original study, which is openly available in the NCBI's GEO database gene repository for rats under accession number GSM4415261. The derived datasets supporting the conclusions of this article will be made available by the authors on request. All the Supplementary Tables and the developed rat genome-scale model files are provided as part of the supplementary data and can be found at the following link (http://datadryad.org/stash/share/RM9HKUOf8PCb-STlufXehShPuXyTbRenn7i_Cl6bmIQ).

References

AbdulHameed M, Liu R, Schyman P, Sachs D, Xu Z, Desai V, Wallqvist A. 2021. ToxProfiler: toxicity-target profiler based on chemical similarity. Comp Toxicol. 18:100162.

Al-Eryani L, Wahlang B, Falkner KC, Guardiola JJ, Clair HB, Prough RA, Cave M. 2015. Identification of environmental chemicals associated with the development of toxicant-associated fatty liver disease in rodents. Toxicol Pathol. 43:482–497.

Baffy G, Brunt EM, Caldwell SH. 2012. Hepatocellular carcinoma in non-alcoholic fatty liver disease: an emerging menace. J Hepatol. 56:1384–1391.

Basaranoglu M, Basaranoglu G, Senturk H. 2013. From fatty liver to fibrosis: a tale of "second hit". World J Gastroenterol. 19:1158–1165.

Beck KR, Sommer TJ, Schuster D, Odermatt A. 2016. Evaluation of tetrabromobisphenol a effects on human glucocorticoid and androgen receptors: a comparison of results from human- with yeast-based *in vitro* assays. Toxicology. 370:70–77.

Benedict M, Zhang X. 2017. Non-alcoholic fatty liver disease: an expanded review. World J Hepatol. 9:715–732.

Blais EM, Rawls KD, Dougherty BV, Li ZI, Kolling GL, Ye P, Wallqvist A, Papin JA. 2017. Reconciled rat and human metabolic networks for comparative toxicogenomics and biomarker predictions. Nat Commun. 8:14250.

Brunk E, Sahoo S, Zielinski DC, Altunkaya A, Drager A, Mih N, Gatto F, Nilsson A, Preciat Gonzalez GA, Aurich MK, et al. 2018. Recon3D enables a three-dimensional view of gene variation in human metabolism. Nat Biotechnol. 36:272–281.

Byass P. 2014. The global burden of liver disease: a challenge for methods and for public health. BMC Med. 12:159.

Carbonell P, Lopez O, Amberg A, Pastor M, Sanz F. 2017. Hepatotoxicity prediction by systems biology modeling of disturbed metabolic pathways using gene expression data. ALTEX. 34:219–234.

Cave M, Falkner KC, Ray M, Joshi-Barve S, Brock G, Khan R, Bon Homme M, McClain CJ. 2010. Toxicant-associated steatohepatitis in vinyl chloride workers. Hepatology. 51:474–481.

Chen KW, Chen YS, Chen PJ, Yeh SH. 2022. Androgen receptor functions in pericentral hepatocytes to decrease gluconeogenesis and avoid hyperglycemia and obesity in male mice. Metabolism. 135:155269.

Committee ES, More SJ, Bampidis V, Benford D, Bennekou SH, Bragard C, Halldorsson TI, Hernandez-Jerez AF, Koutsoumanis K, Naegeli H, *et al.* 2019. Guidance on harmonised methodologies for human health, animal health and ecological risk assessment of combined exposure to multiple chemicals. EFSA J. 17:e05634.

Corless JK, Middleton HM III. 1983. Normal liver function. A basis for understanding hepatic disease. Arch Intern Med. 143:2291–2294.

Ganter B, Snyder RD, Halbert DN, Lee MD. 2006. Toxicogenomics in drug discovery and development: mechanistic analysis of compound/class-dependent effects using the DrugMatrix database. Pharmacogenomics. 7:1025–1044.

Gille C, Bolling C, Hoppe A, Bulik S, Hoffmann S, Hubner K, Karlstadt A, Ganeshan R, Konig M, Rother K, *et al.* 2010. HepatoNet1: a comprehensive metabolic reconstruction of the human hepatocyte for the analysis of liver physiology. Mol Syst Biol. 6:411.

Gwinn WM, Auerbach SS, Parham F, Stout MD, Waidyanatha S, Mutlu E, Collins B, Paules RS, Merrick BA, Ferguson S, *et al.* 2020. Evaluation of 5-day *in vivo* rat liver and kidney with high-throughput transcriptomics for estimating benchmark doses of apical outcomes. Toxicol Sci. 176:343–354.

Han H, Cho JW, Lee S, Yun A, Kim H, Bae D, Yang S, Kim CY, Lee M, Kim E, *et al.* 2018. TRRUST v2: an expanded reference database of human and mouse transcriptional regulatory interactions. Nucleic Acids Res. 46:D380–D386.

Heirendt L, Arreckx S, Pfau T, Mendoza SN, Richelle A, Heinken A, Haraldsdottir HS, Wachowiak J, Keating SM, Vlasov V, *et al.* 2019. Creation and analysis of biochemical constraint-based models using the COBRA toolbox v.3.0. Nat Protoc. 14:639–702.

Huang DW, Sherman BT, Stephens R, Baseler MW, Lane HC, Lempicki RA. 2008. DAVID gene ID conversion tool. Bioinformation. 2:428–430.

Igarashi Y, Nakatsu N, Yamashita T, Ono A, Ohno Y, Urushidani T, Yamada H. 2015. Open TG-GATEs: a large-scale toxicogenomics database. Nucleic Acids Res. 43:D921–D927.

Jones JG. 2016. Hepatic glucose and lipid metabolism. Diabetologia. 59:1098–1103.

Karp PD, Midford PE, Caspi R, Khodursky A. 2021. Pathway size matters: the influence of pathway granularity on over-representation (enrichment analysis) statistics. BMC Genomics. 22:191.

Kharlyngdoh JB, Pradhan A, Olsson PE. 2018. Androgen receptor modulation following combination exposure to brominated flame-retardants. Sci Rep. 8:4843.

Kiani AK, Pheby D, Henehan G, Brown R, Sieving P, Sykora P, Marks R, Falsini B, Capodicasa N, Miertus S, *et al.* 2022. Ethical considerations regarding animal experimentation. J Prev Med Hyg. 63(2 Suppl 3):E255–E266.

Leung TM, Nieto N. 2013. CYP2E1 and oxidant stress in alcoholic and non-alcoholic fatty liver disease. J Hepatol. 58:395–398.

Liu RJ, He YJ, Liu H, Zheng DD, Huang SW, Liu CH. 2021. Protective effect of *Lycium barbarum* polysaccharide on di-(2-ethylhexyl)

phthalate-induced toxicity in rat liver. Environ Sci Pollut Res Int. 28:23501–23509.

Mackowiak B, Hodge J, Stern S, Wang H. 2018. The roles of xenobiotic receptors: beyond chemical disposition. Drug Metab Dispos. 46:1361–1371.

Mardinoglu A, Agren R, Kampf C, Asplund A, Nookaew I, Jacobson P, Walley AJ, Froguel P, Carlsson LM, Uhlen M, *et al.* 2013. Integration of clinical data with a genome-scale metabolic model of the human adipocyte. Mol Syst Biol. 9:649.

Maronpot RR, Yoshizawa K, Nyska A, Harada T, Flake G, Mueller G, Singh B, Ward JM. 2010. Hepatic enzyme induction: histopathology. Toxicol Pathol. 38:776–795.

Nguyen TM, Shafi A, Nguyen T, Draghici S. 2019. Identifying significantly impacted pathways: a comprehensive review and assessment. Genome Biol. 20:203.

Nielsen J. 2009. Systems biology of lipid metabolism: from yeast to human. FEBS Lett. 583:3905–3913.

OECD. 1994. OECD guidelines for the testing of chemicals. Paris: Organization for Economic Co-Operation and Development.

Padda MS, Sanchez M, Akhtar AJ, Boyer JL. 2011. Drug-induced cholestasis. Hepatology. 53:1377–1387.

Pannala VR, Balik-Meisner MR, Mav D, Phadke DP, Scholl EH, Shah RR, Auerbach SS, Wallqvist A. 2023. High-throughput transcriptomics differentiates toxic versus non-toxic chemical exposures using a rat liver model. Int J Mol Sci. 24:17425.

Pannala VR, Estes SK, Rahim M, Trenary I, O'Brien TP, Shiota C, Printz RL, Reifman J, Oyama T, Shiota M, *et al.* 2020a. Mechanism-based identification of plasma metabolites associated with liver toxicity. Toxicology. 441:152493.

Pannala VR, Estes SK, Rahim M, Trenary I, O'Brien TP, Shiota C, Printz RL, Reifman J, Shiota M, Young JD, *et al.* 2020b. Toxicant-induced metabolic alterations in lipid and amino acid pathways are predictive of acute liver toxicity in rats. Int J Mol Sci. 21:8250.

Pannala VR, Vinnakota KC, Estes SK, Trenary I, O'Brien TP, Printz RL, Papin JA, Reifman J, Oyama T, Shiota M, *et al.* 2020c. Genome-scale model-based identification of metabolite indicators for early detection of kidney toxicity. Toxicol Sci. 173:293–312.

Pannala VR, Vinnakota KC, Rawls KD, Estes SK, O'Brien TP, Printz RL, Papin JA, Reifman J, Shiota M, Young JD, *et al.* 2019. Mechanistic identification of biofluid metabolite changes as markers of acetaminophen-induced liver toxicity in rats. Toxicol Appl Pharmacol. 372:19–32.

Pannala VR, Wall ML, Estes SK, Trenary I, O'Brien TP, Printz RL, Vinnakota KC, Reifman J, Shiota M, Young JD, *et al.* 2018. Metabolic network-based predictions of toxicant-induced metabolite changes in the laboratory rat. Sci Rep. 8:11678.

Pond SM. 1982. Effects on the liver of chemicals encountered in the workplace. West J Med. 137:506–514.

Ramaiahgari SC, Auerbach SS, Saddler TO, Rice JR, Dunlap PE, Sipes NS, DeVito MJ, Shah RR, Bushel PR, Merrick BA, *et al.* 2019. The power of resolution: contextualized understanding of biological responses to liver injury chemicals using high-throughput transcriptomics and benchmark concentration modeling. Toxicol Sci. 169:553–566.

Rawls KD, Dougherty BV, Vinnakota KC, Pannala VR, Wallqvist A, Kolling GL, Papin JA. 2021. Predicting changes in renal metabolism after compound exposure with a genome-scale metabolic model. Toxicol Appl Pharmacol. 412:115390.

Regev A. 2014. Drug-induced liver injury and drug development: industry perspective. Semin Liver Dis. 34:227–239.

Seeff LB. 2015. Drug-induced liver injury is a major risk for new drugs. Dig Dis. 33:458–463.

Tawa GJ, AbdulHameed MD, Yu X, Kumar K, Ippolito DL, Lewis JA, Stallings JD, Wallqvist A. 2014. Characterization of chemically induced liver injuries using gene co-expression modules. PLoS One. 9:e107230.

Terzer M, Maynard ND, Covert MW, Stelling J. 2009. Genome-scale metabolic networks. Wiley Interdiscip Rev Syst Biol Med. 1:285–297.

Thiele I, Palsson BO. 2010. A protocol for generating a high-quality genome-scale metabolic reconstruction. Nat Protoc. 5:93–121.

Tolman KG, Sirrine RW. 1998. Occupational hepatotoxicity. Clin Liver Dis. 2:563–589.

Van Norman GA. 2019. Limitations of animal studies for predicting toxicity in clinical trials: is it time to rethink our current approach? JACC Basic Transl Sci. 4:845–854.

Wang H, Robinson JL, Kocabas P, Gustafsson J, Anton M, Cholley PE, Huang S, Gobom J, Svensson T, Uhlen M, *et al.* 2021. Genome-scale metabolic network reconstruction of model animals as a platform for translational research. Proc Natl Acad Sci USA. 118: e2102344118.

Yu C, Woo HJ, Yu X, Oyama T, Wallqvist A, Reifman J. 2017. A strategy for evaluating pathway analysis methods. BMC Bioinformatics. 18:453.